Bifurcations of the dark soliton and polarization domain walls in nonlinear dispersive media

M. Haelterman and A. P. Sheppard
Optical Sciences Center, Australian National University, Canberra, Australia
(Received 20 August 1993; revised manuscript received 28 December 1993)

A bifurcation analysis of the coupled nonlinear Schrödinger equations that govern light propagation in Kerr media reveals the existence of a novel type of vector dark solitary waves. These solutions consist of a localized structure separating two uniform background waves of the same amplitude but opposite circular polarizations and constitute therefore polarization domain walls.

PACS number(s): 42.81.Dp, 42.81.Gs, 03.40.Kf

In the context of optics the nonlinear Schrödinger (NLS) equation describes one-dimensional light propagation in dispersive Kerr media such as single-mode optical fibers. The fundamental bright soliton solution to this integrable equation [1] represents an ultrashort light pulse which propagates without distortion in the anomalous regime of group velocity dispersion [2]. In the case of normal group velocity dispersion the NLS equation possesses dark soliton solution which consists of a localized structure separating two uniform background waves of identical amplitude but of different phases [3,4]. In the spatial domain, the NLS equation also describes nonlinear propagation of two-dimensional (2D) cw laser beams in diffractive Kerr materials [1]. In this context, the bright soliton occurs in self-focusing media and consists of a self-guided laser beam whose transverse envelope is the fundamental guided mode of the waveguide it induces through the nonlinearity [5], whereas a dark soliton beam is the second mode at cutoff of the waveguide it induces in a self-defocusing Kerr medium [5].

Being derived in the scalar approximation of the electromagnetic field, the NLS equation only describes light pulses or 2D laser beams with a uniform and constant polarization. However, in practice the polarization components of the field constitute two interdependent optical modes subject to important linear and nonlinear interactions (see, e.g., the review paper, Ref. [6]). In the presence of more than one optical mode the propagation of light in dispersive or diffractive Kerr media is described by a set of coupled NLS equations.

Coupled NLS equations describe phenomena of common occurrence in nonlinear optics [7] as well as in plasma physics [8] where their study revealed an extremely rich spectrum of complex behaviors. In nonlinear optics special attention has been paid to polarized soliton interaction in birefringent materials where the interplay of linear and nonlinear coupling leads to intriguing phenomena. In particular, it was shown in the anomalous dispersion regime that solitons belonging to two polarization modes may form a stationary bound state (vector solitary wave) [9,10]. This type of solutions to the coupled NLS equations was later analyzed in terms of bifurcations of polarized bright NLS solitons [11,12]. Several studies have also been devoted to the problem of bright and dark soliton pairing considering both dispersion regimes (see, e.g., Refs. [13,14]). In a recent work, Kivshar and Turitsyn showed the existence of a new type of vector dark solitary waves in the normal dispersion regime [15]. These solitary waves are bound states of two gray solitons of different amplitudes and orthogonal polarizations.

The purpose of this paper is to analyze hitherto unrecognized bifurcations of the coupled NLS equations and to present a novel class of dark vector solitary waves. We show analytically and numerically that these new solitary waves constitute the limiting states of branches of solutions which bifurcate from the circularly polarized fundamental NLS dark soliton. They consist of localized structures separating two circularly polarized uniform background waves of the same amplitude but opposite handedness. They can therefore be viewed as polarization domain walls.

In normalized units the circular polarization components of the field propagating in an isotropic Kerr medium are given by the coupled NLS equations (see, e.g., Ref. [15])

$$i\frac{\partial U}{\partial z}-\frac{1}{2}\frac{\partial^2 U}{\partial \xi^2}+(|U|^2+\sigma|V|^2)U=0\ , \tag{1a}$$

$$i\frac{\partial V}{\partial z}-\frac{1}{2}\frac{\partial^2 V}{\partial \xi^2}+(|V|^2+\sigma|U|^2)V=0\ , \tag{1b}$$

where $U(z,\xi)$ and $V(z,\xi)$ are the envelopes of both polarization components and σ is the cross-phase modulation (CPM) coefficient defined as $\sigma=(1+B)/(1-B)$ with $B=\chi^{(3)}_{1221}/\chi^{(3)}_{1111}$ where $\chi^{(3)}_{ijkl}$ is the nonlinear susceptibility tensor of the material [16]. The coordinate ξ is either the time coordinate in a reference frame traveling at the group velocity of light (temporal domain) or the transverse spatial coordinate of a 2D beam (spatial domain). Note that according to the sign of the second derivative in ξ in Eq. (1), we restrict our developments to the cases of pulse propagation in the normal dispersion regime (with positive Kerr nonlinearity) and 2D beam propagation in self-defocusing media.

Equation (1) admits as solution the circularly polarized dark soliton

$$U(z,\xi)=\sqrt{\alpha}\tanh(\sqrt{\alpha}\xi)\exp(i\alpha z),\quad V(z,\xi)=0\ . \tag{2}$$

In the following we will study bifurcations of this simple and well-known solution. Before doing so, it is con-

venient to investigate its stability by means of a standard linear stability analysis. To this end we introduce the ansatz

$$U(z,\xi)=[\sqrt{\alpha}\tanh(\sqrt{\alpha}\xi)\exp(i\alpha z)+u],\quad V(z,\xi)=v \tag{3}$$

where u and v are the linear perturbations in both polarization components. Substituting Eq. (3) into Eq. (1) leads to two decoupled linear equations in u and v,

$$i\frac{\partial u}{\partial z}-\frac{1}{2}\frac{\partial^2 u}{\partial \xi^2}-\alpha u+\alpha\tanh^2(\sqrt{\alpha}\xi)(2u+u^*)=0\ , \tag{4a}$$

$$i\frac{\partial v}{\partial z}-\frac{1}{2}\frac{\partial^2 v}{\partial \xi^2}+\sigma\alpha\tanh^2(\sqrt{\alpha}\xi)v=0\ . \tag{4b}$$

The independence of u and v makes the stability analysis very simple. Equation (4a) is nothing but the equation of the linear stability analysis of the scalar dark soliton [17,18]. The result of this analysis is well known; it merely shows that the scalar dark soliton is unconditionally stable. As a consequence, only Eq. (4b), i.e., the presence of the second polarization component, could lead to the instability of the dark soliton. The stability is investigated by introducing the usual ansatz $v=y(\xi)\exp(\lambda z)$, where λ is the growth rate of the arbitrary initial linear perturbation $y(\xi)$. This leads to the equation

$$\tfrac{1}{2}\ddot{y}-\sigma\alpha\tanh^2(\sqrt{\alpha}\xi)y=i\lambda y\ , \tag{5}$$

where the dot denotes derivative with respect to ξ. This eigenvalue equation is well known in optical waveguide theory; it is the modal equation of the sech^2 index profile planar waveguide [19]. The complex number $i\lambda$ represents the propagation constant of a given mode, say $\beta=-i\lambda$. The propagation constant β associated with any bound function $y(\xi)$ (i.e., either guided or radiation modes) is real and positive [19]. This means that all the eigenvalues of Eq. (4b) have a zero imaginary part, $\mathrm{Re}(\lambda)=0$. In other words, the linear perturbation growth rate is always zero. Such a result indicates that the circularly polarized dark soliton is neutrally stable with respect to a perturbation of its polarization state. A perturbation in V does not grow or decay and propagates with the dark soliton in U. This behavior is a direct consequence of the energy conservation law of Eq. (1b), i.e., $\partial_z[\int_{-\infty}^{+\infty}|V|^2 d\xi]=0$.

The conclusion of this linear stability analysis can be easily interpreted by means of optical waveguide theory. A spatial dark soliton in the field U induces a waveguide for the field V (through CPM) and any initial distribution of the field V of arbitrarily small amplitude can be decomposed into the guided and radiation modes of this waveguide. These modes propagate along z without loss, which corresponds to the neutral stability of the circularly polarized dark soliton. Of course, only the guided modes in V propagate along the axis of the dark soliton in U and are liable to form a bound state of both polarizations. If the initial perturbation is such that only one guided mode is excited, the resulting polarization bound state is stationary. Note that theoretical and experimental studies of CPM-induced waveguiding have already been reported in the literature in the case of beams of different frequencies (see, e.g., [20,21]).

From this reasoning we anticipate that when the power in the guided mode V is increased into the nonlinear regime, the bound state can still exist at the expense of a reshaping of the profile of the dark soliton in U. The resulting bound states would therefore constitute a new family of vector solitary waves which branches from the circularly polarized dark soliton solution given in Eq. (2). The branching point corresponds to the linear regime of the guided mode in V. For each guided mode of the CPM-induced waveguide we can expect a branching bifurcation from the circularly polarized dark NLS soliton.

Being composed of mutually trapped waveguide modes, the new solitary-wave solutions have the form

$$\begin{aligned} U(z,\xi)&=u(\xi)\exp(i\alpha z)\ ,\\ V(z,\xi)&=v(\xi)\exp(i\beta z)\ , \end{aligned} \tag{6}$$

where the envelopes u,v and the corresponding propagation constants α,β are real. Substituting these forms of U and V into Eq. (1) leads to a set of coupled ordinary differential equations

$$\tfrac{1}{2}\ddot{u}+\alpha u-u^3-\sigma v^2 u=0\ , \tag{7a}$$

$$\tfrac{1}{2}\ddot{v}+\beta v-v^3-\sigma u^2 v=0\ . \tag{7b}$$

Equation (7) is the equation of motion in the (u,v) plane of a unit mass in the potential

$$\mathcal{V}(u,v)=\alpha u^2+\beta v^2-\tfrac{1}{2}(u^4+v^4)-\sigma u^2 v^2\ . \tag{8}$$

The solitary-wave solutions to Eq. (7) correspond to the separatrix trajectories of this potential. It is easy to see from Eq. (8) that $\mathcal{V}$ possesses four maxima on the u and v axes. The separatrices that connect the pairs of opposite maxima correspond to the circularly polarized NLS dark solitons. These solutions are

$$u=\sqrt{\alpha}\tanh(\sqrt{\alpha}\xi),\quad v=0\ , \tag{9a}$$

$$u=0,\quad v=\sqrt{\beta}\tanh(\sqrt{\beta}\xi)\ . \tag{9b}$$

In order to study the bifurcations of the circularly polarized soliton we follow the procedure of Refs. [11,12]. Let us consider the solution of Eq. (7) as a soliton (9a) plus a small perturbation, that is,

$$u=\sqrt{\alpha}\tanh(\sqrt{\alpha}\xi)+\varepsilon^2 x\ , \tag{10a}$$

$$v=\varepsilon y\ . \tag{10b}$$

It is easy to verify from Eq. (7) that the linear term in ε in Eq. (10a) is zero. Substituting Eq. (10) into Eq. (7) we obtain, to the leading order, two decoupled equations in x and y. The equation in y is

$$\tfrac{1}{2}\ddot{y}+\beta y-\sigma\alpha\tanh^2(\sqrt{\alpha}\xi)y=0\ . \tag{11}$$

The solutions to this linear eigenvalue problem are well known in optical waveguide theory since it constitutes the modal equation of the sech^2 index profile planar waveguide [19]. Because the opposite maxima corresponding to the separatrices of $\mathcal{V}$ are on the u and v axes, we must restrict this eigenvalue problem to the solutions $y(\xi)$ that decay at $\xi=\pm\infty$. Choosing the value $\sigma=2$

which corresponds to the nonlinearity of silica fibers, we then find two solutions (corresponding to the two guided modes of the CPM-induced waveguide) [19]

$$y_0=\mathrm{sech}^{\nu}(\sqrt{\alpha}\xi) \quad \text{at } \beta=\beta_0=0.78\alpha\ , \tag{12a}$$

$$y_1=P_{\nu}^{1-\nu}[\tanh(\sqrt{\alpha}\xi)] \quad \text{at } \beta=\beta_1=1.84\alpha\ , \tag{12b}$$

where P_{ν}^{μ} is the Legendre function of the first kind and $\nu=1.56$. Equation (12a) reveals the existence of a bifurcation at $\beta=\beta_0=0.78\alpha$. This bifurcation corresponds to a branch of bound solitary-wave solutions u,v in which v is a symmetric function, it is then characterized by a change of symmetry in the total field (u being an antisymmetric function). Equation (12a) represents the fundamental mode of the waveguide seen by the wave V in the linear regime and β_0 is its propagation constant. The associated bifurcation branch will be found for values of β corresponding to an increase in the power of V. These solutions can easily be calculated numerically from Eq. (7) using a standard shooting method. Their symmetry is such that $\dot{v}=0$ on the v axis ($u=0$); it is therefore convenient to choose the value of v on this axis, say v_0, as the shooting parameter (the value of $\dot{u}$ is then found from the energy conservation law of the unit mass motion). Figure 1 shows the evolution of the separatrices, as β tends from β_0 to α, and the corresponding bifurcation diagram. Note that Eq. (7) can be normalized with respect to α, and in the following we can set α equal to unity without loss of generality. In Fig. 2 we plotted the envelopes of the polarization components $u(\xi)$ and $v(\xi)$ that correspond to this new bifurcation branch. We see that as β increases from β_0 a pulse grows in the component v around the origin; in the same region, the slope of wave u decreases. When β approaches α, two pairs of bound kink waves are formed, separating regions of orthogonal circular polarization states (i.e., regions in which either U or V is zero). As β tends to α the distance between these localized structures increases indefinitely and the pairs of bound kink waves appear as being independent localized structures of the field. In other words, they constitute vector solitary waves of the dark type (nonvanishing boundary conditions) separating domains of orthogonal polarizations. The existence of such coupled kink waves can be easily understood from the analysis of the potential $\mathcal{V}$.

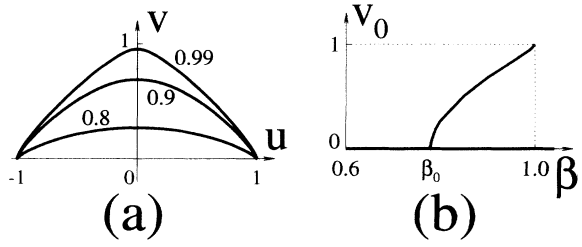

FIG. 1. (a) Separatrix trajectories for different values of β (and $\alpha=1$). These values are indicated on the curves. (b) The corresponding bifurcation diagram $v_0(\beta)$. Note that the thick line on the axis $v_0=0$ represents the branch of the circularly polarized NLS soliton.

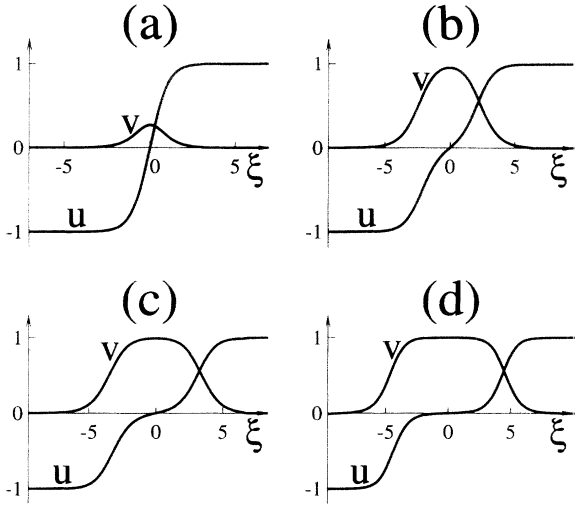

FIG. 2. Bound solitary-wave envelopes u and v corresponding to the bifurcation branch of Fig. 1. Curves are given for different values of $\varepsilon=\alpha-\beta$, (a) $\varepsilon=0.2$, (b) $\varepsilon=0.05$, (c) $\varepsilon=10^{-3}$, (d) $\varepsilon=10^{-5}$.

Before doing the analysis of these localized structures let us consider the stability of the solutions of the new bifurcation branch illustrated in Figs. 1 and 2. First note that the bifurcation does not affect the stability of the branch of the circularly polarized dark soliton. As we have seen above, the dark soliton is always neutrally stable with respect to perturbations of its polarization state. Since we do not have analytical expressions for the new vector solitary waves, the stability of the second branch must be investigated numerically. We have performed numerical simulations of the propagation equation [Eq. (1)] with the solitary waves of Fig. 2 as initial conditions. We verified their stability with respect to several types of perturbations. Figure 3 illustrates the stability with respect to large amplitude perturbations. The initial condition is given by an approximation of the profiles of the solitary waves $u(\xi),v(\xi)$ by Gaussian functions: $u(\xi)=1-\exp(-a\xi^2)$ for $\xi>0, u(\xi)=\exp(-a\xi^2)-1$ for $\xi<0$, and $v(\xi)=\exp(-a\xi^2)$, where the parameter a is adjusted to the width of the solitary wave of Fig. 2(b); $a=0.36$. We see in Fig. 3(a) that after oscillation and emission of radiation the field settles down to a stationary steady state. This state is identified as being a solitary-wave solution whose parameter β is close to the one of Fig. 2(b) [due to the radiation loss the final intensity in V is slightly smaller than in the case of Fig. 2(b) and $\beta\approx 0.93$]. Figure 3(b) shows the initial (dotted lines) and the final steady-state (solid lines) intensity profiles of both polarization components. This result illustrates the robust nature of the vector solitary waves which originate from the dark NLS soliton bifurcation associated with the fundamental mode of the CPM-induced waveguide.

To illustrate the importance of the bifurcation of the circularly polarized dark NLS soliton we have performed the numerical simulation of the propagation of the dark soliton through an amplifier. The situation is idealized

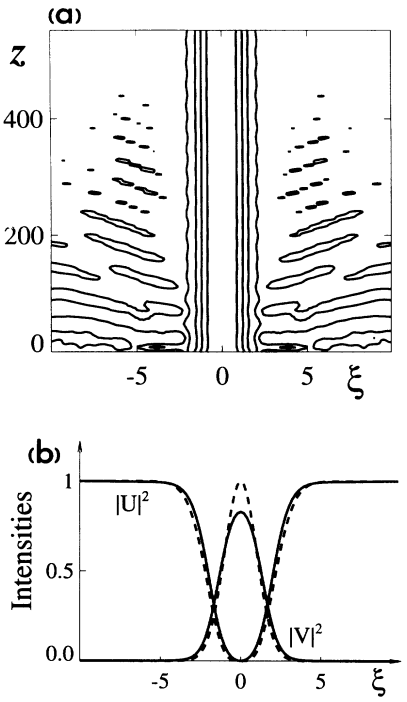

FIG. 3. Numerical simulation of the propagation of a perturbed solitary wave of the new solution branch. The initial field envelopes are given in the text. (a) Contour plot of the intensity $|U(\xi,z)|^2$ (note that in order to avoid reflection of the radiation on the edges of the numerical window, broad radiation damping regions have been introduced at each extremity of the window). (b) Initial (dotted lines) and final (solid lines) intensity profiles of both polarization components.

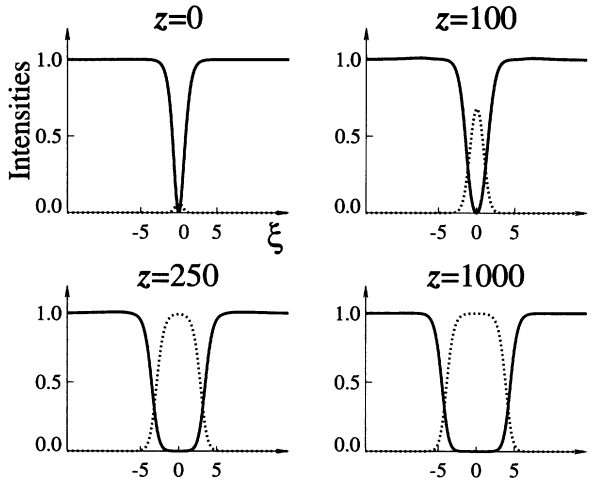

FIG. 4. Evolution of the intensity profiles, $|U|^2$ (solid line) and $|V|^2$ (dotted line), obtained when the polarization component V is adiabatically amplified. The initial conditions are described in the text. We clearly verify the formation of the solitary waves of the new solution branch of Figs. 1 and 2.

by considering a selective amplification of one circular polarization component only (we do not discuss here the different possible ways to get such a feature in practice). We simply assume that the component U of the dark soliton is not affected by the amplifier and that the component V undergoes adiabatic amplification. The initial condition corresponds to a dark NLS soliton for the field U and a small amplitude Gaussian envelope centered on the soliton for the polarization component V. The intensity of the initial Gaussian beam (or pulse) is one-tenth of the dark soliton intensity. Figure 4 shows the evolution of the intensity profiles of both fields during propagation. We see that, while the intensity in V increases, the dark soliton broadens and exhibits a flat region of zero intensity around the origin $\xi=0$. The intensity in V saturates when it approaches unity and after $z\approx 250$ the effect of amplification only results in a broadening of the field profile. As a result, the intensity profiles in both polarization components acquire a square shape and two distinct pairs of kink waves are formed. In fact, this scenario reproduces the evolution of the solitary-wave solutions along the bifurcation branch studied above (compare Fig. 4 with Fig. 2). This simulation also confirms the stability of these solitary waves.

Let us now study the kink solitary waves observed in the limit $\beta\rightarrow\alpha$ of the new solitary-wave solution branch. Their existence can be easily explained by means of an analysis of the potential $\mathcal{V}(u,v)$. In Fig. 5 we show a contour plot of $\mathcal{V}(u,v)$ in the particular case where $\beta=\alpha$ and $\sigma=2$. The separatrices are the trajectories that connect pairs of saddle points or maxima of this potential. The thick solid lines in Fig. 5 connect opposite maxima. They naturally correspond to the circularly polarized dark solitons. The dashed trajectories in Fig. 5 connect opposite saddle points. They correspond to the linearly polarized dark solitons $u=\pm v=\sqrt{1/(1+\sigma)}\tanh(\xi)$ easily derived from Eq. (7) when setting $\beta=\alpha=1$ and $u=\pm v$. The dotted lines in Fig. 5 show the four separatrices that connect adjacent maxima of the potential $\mathcal{V}$. They have been calculated numerically from Eq. (7) which is in general nonintegrable [12]. The solitary-wave envelopes $u(\xi)$ and $v(\xi)$ corresponding to the separatrix of the first quadrant $(u,v>0)$ are shown in Fig. 6(a) (the envelopes of

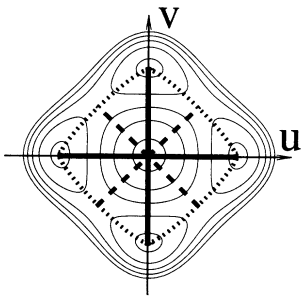

FIG. 5. Contour plot of the potential $\mathcal{V}$ in the (u,v) plane in the limiting case where $\beta=\alpha=1$ [the positions of the maxima of $\mathcal{V}$ are $(\pm 1,0)$ and $(0,\pm 1)$]. The solid and dashed lines show the separatrices of the circularly and linearly polarized NLS dark solitons, respectively. The dotted lines connect the four adjacent maxima of the potential. They are the separatrices of the polarization domain walls.

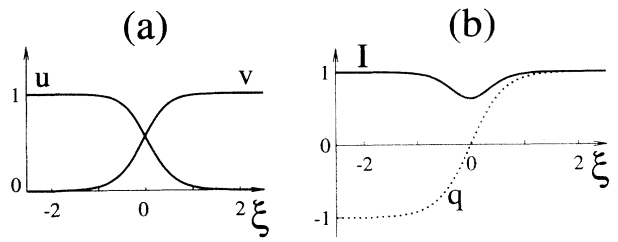

FIG. 6. (a) Circular polarization envelopes u and v of the polarization domain wall. (b) Total intensity profile $I(\xi)$ and ellipticity degree $q(\xi)$ of the polarization domain wall.

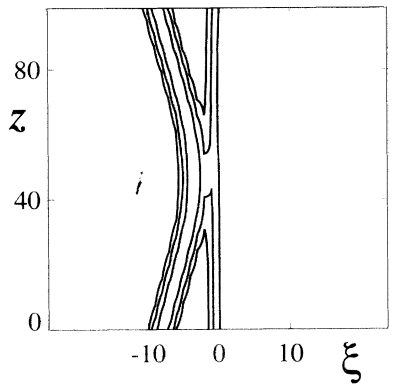

FIG. 7. Numerical simulation of the collision between a gray soliton and a polarization domain wall. The graph shows the contour lines of the intensity profile $|U(\xi,z)|^2$. The gray soliton is introduced in the field U and its phase and amplitudes are adjusted to match the field of the polarization domain wall of amplitude equal to unity [see Fig. 6(a)]. The phase parameter of the gray soliton is $\phi=\frac{1}{8}$.

the separatrices of the other quadrants only differ by changes of the signs of u and v). We clearly recognize the kink shape of the waves of Fig. 2(d). As illustrated in Fig. 6(b), the total intensity profile, $I(\xi)=u(\xi)^2+v(\xi)^2$, consists of a dark pulse inscribed onto a constant background. In Fig. 6(b) we also plotted the ellipticity degree of the total field, $q=(u-v)/(u+v)$. The values $q=+1$ and -1 correspond to circular polarization states of opposite handedness, while $q=0$ corresponds to a linear polarization state. We see that the bound kink solitary waves u and v form a localized structure consisting of a dip in a constant intensity background accompanied by a progressive inversion of the ellipticity of the field. Since this localized structure connects two domains of orthogonal stable eigenpolarizations of the Kerr medium [16] it can be called a polarization domain wall. Let us note, finally, that the existence of such polarization domain walls is closely related to the tensor character of the Kerr nonlinearity. It is, in fact, easy to see from Eq. (8) that the potential $\mathcal{V}$ possesses maxima on the u and v axes only if $\sigma>1$ (i.e., $\chi^{(3)}_{1221}\neq 0$). The σ dependence of $\mathcal{V}$ indicates that, for a given intensity, the smaller σ the broader the domain walls. In the limit $\sigma\to 1$ their width becomes infinite.

We have checked the propagation stability of the polarization domain walls by numerical simulations of Eq. (1). As for the compound solitary waves studied above, we have verified their stability with respect to large perturbations. Figure 7 illustrates a quite drastic stability test. It shows, in the form of a contour plot of the intensity of the field U, the collision of a polarization domain wall (located in $\xi=0$) with a gray soliton. The general form of the gray soliton solution of the NLS equation is $u_0\{\cos\phi\tanh[\eta(\xi-\Omega z)]-i\sin\phi\}$ where $\Omega=|u_0|\sin\phi$ and $\eta=|u_0|\cos\phi$ [15]. In order to match the fields of the gray soliton and the polarization domain wall we have to choose $u_0=\exp(i\phi)$ (the amplitude of the domain wall is real and equal to unity). For the example of Fig. 7 the transverse velocity $\Omega=\sin\phi$ of the gray soliton is determined by the value $\phi=\frac{1}{8}$, which corresponds to a total phase change of $\pi-2\phi=0.92\pi$ across the gray soliton width. This represents a perturbation of almost twice the amplitude of the domain wall itself. We see, however, that this large perturbation does not affect the domain wall. The grey soliton simply bounces back during the collision and the shape and trajectory of the domain wall remain almost unchanged. Analogous results, obtained with other types of perturbations, confirmed this robust solitonlike nature of the polarization domain walls.

To a certain extent these solitary waves are qualitatively similar to the polarization domain walls studied by Zakharov and Mikhailov in Ref. [22]. In that case, however, the localized structures result from the nonlinear interaction between two counterpropagating beams of orthogonal polarizations in a dispersionless Kerr material. In fact, the localized structures of Ref. [22] separate orthogonal eigenpolarizations of systems of counterpropagating waves. Such polarization eigenstates are discussed in detail in Ref. [23]. In our case the localized structures separate orthogonal eigenpolarizations of single wave systems [16] (here, since we restricted our analysis to isotropic media, these eigenpolarizations are the linear and the circular polarization states). Of course, the physical situation as well as the mathematical model considered in Ref. [22] have no connection with the present case and the similarity is limited to the simple fact that both situations involve localized structures separating uniform eigenpolarization domains in a Kerr material. To be more precise and to differentiate the vector kink solitary waves considered here from the solitary waves of Ref. [22], one should call them "diffractive" or "dispersive" polarization domain walls depending on whether we consider the spatial or the temporal domain.

An interesting parallel can also be drawn from a topological point of view between the polarization domain walls considered here and a new class of localized structures in discrete models of solids recently reported in the literature [24,25]. In this latter case the localized structures separate domains of symmetric lattice vibration eigenmodes.

The solitary waves u and v of the first bifurcation branch represented in Fig. 2 can now be viewed as bound states of polarization domain walls. We see in Fig. 1(a) that, in the limit $\beta\to\alpha$, the separatrix trajectory tends to the two separatrices of the domain walls of the first and

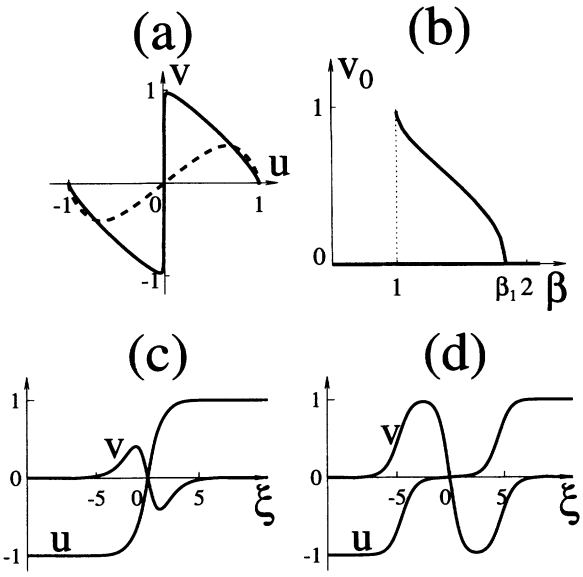

FIG. 8. (a) Two separatrix trajectories of the second bifurcation branch, the values of β corresponding to the dotted and solid lines are $\beta=1.6$ and $\beta=1.002$, respectively. (b) The corresponding bifurcation diagram, and (c) and (d) the envelopes u and v of the separatrices shown in (a).

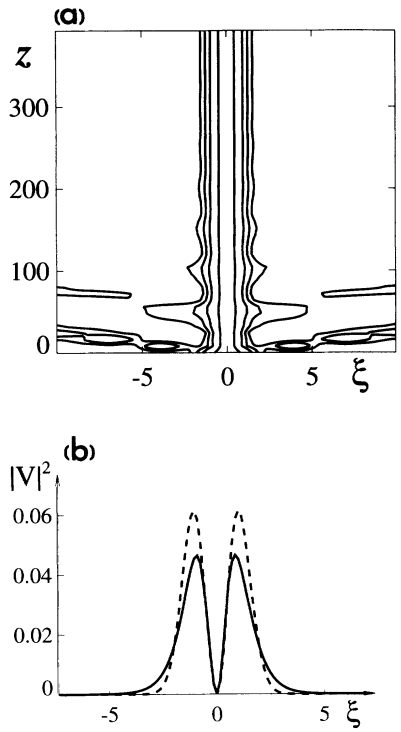

FIG. 9. Numerical simulation of the propagation of a perturbed solitary wave of the second solution branch. The initial field envelopes are given in the text. (a) Contour plot of the intensity $|U(\xi,z)|^2$. (b) Initial (dotted lines) and final (solid lines) intensity profiles of the polarization component V.

second quadrants shown in Fig. 5. At this stage the total field is then composed of two independent (i.e., infinitely far apart) domain walls. As β decreases the domain walls rapidly come closer to one another and form a stationary bound state. When β approaches β_0 the two domain walls coalesce and in the limit $\beta=\beta_0$ they finally form a simple dark NLS soliton.

The second bifurcation revealed by the solution (12b) is more complex. It occurs at $\beta=\beta_1=1.84\alpha$ and since the corresponding guided mode y_1 is antisymmetric it does not involve a change of the symmetry of the total field. Figure 8 shows two examples of separatrix trajectories, the corresponding solitary-wave envelopes as well as the bifurcation diagram (v_0 now denotes the maximum value of the amplitude v). Similarly to the first bifurcation, the profile of u flattens around the origin. Here this process is accompanied by the growth of two π out-of-phase pulses in v. As a result, when β approaches α the field distribution is composed of one circularly polarized NLS dark soliton surrounded by two identical polarization domain walls [the trajectory being close to the domain wall separatrices of the first and third quadrants as shown in Fig. 8(a)].

These solutions were also proven to be stable in propagation. In Figs. 9(a) and 9(b) we show the example of a perturbed solitary wave close to the bifurcation. The initial condition for the field U is the dark NLS soliton whereas the initial envelope in V is given by $v(\xi)=a\xi\exp(-b\xi^2)$ where a and b are chosen to approach the amplitude and width of a solitary-wave solution ($a=0.1, b=0.5$). As in the case of Fig. 3, we observe a reshaping of the dark soliton accompanied by radiation and damped oscillations. Both fields U and V rapidly settle down to a steady state identified as being the solitary-wave solution corresponding to the parameter $\beta\approx 1.83$.

In conclusion, we have shown analytically the existence of bifurcations of the dark soliton solutions to the coupled NLS equations. These bifurcations have been explained by means of a simple physical reasoning based on linear optical waveguide theory. The solitary-wave solutions of the corresponding bifurcation branches have been studied numerically. We showed that, far from the bifurcation points, these solutions tend to composite states of independent pairs of kink solitary waves. These waves constitute localized structures separating regions of different eigenpolarizations of the Kerr medium and can therefore be viewed as polarization domain walls. The stability of the polarization domain walls as well as of the compound solitary waves has been investigated by means of numerical simulations of the full dynamical model. All the solutions revealed by the present bifurcations of the dark NLS soliton were proven to be stable. In particular, we showed that the polarization domain walls exhibit a robust solitonlike nature which allows us to consider them as a novel type of fundamental vector solitary waves of Kerr media.

Helpful discussions with Yu. S. Kivshar are gratefully acknowledged. This work has been supported by the Australian Photonics Cooperative Research Centre.

[1] V. E. Zakharov and A. B. Shabat, Zh. Eksp. Teor. Fiz. **61**, 118 (1971) [Sov. Phys. JETP **34**, 62 (1972)].
[2] A. Hasegawa and F. Tappert, Appl. Phys. Lett. **23**, 142 (1973).
[3] V. E. Zakharov and A. B. Shabat, Zh. Eksp. Teor. Fiz. **64**, 1627 (1973) [Sov. Phys. JETP **37**, 823 (1973)].
[4] A. Hasegawa and F. Tappert, Appl. Phys. Lett. **23**, 171 (1973).
[5] A. W. Snyder, L. Poladian, and D. J. Mitchell, Opt. Lett. **17**, 789 (1992).
[6] N. I. Zhedulev, Usp. Fiz. Nauk **157**, 683 (1989) [Sov. Phys. Usp. **32**, 357 (1989)].
[7] See, e.g., G. P. Agrawal, *Nonlinear Fiber Optics* (Academic, New York, 1989).
[8] See, e.g., A. L. Berkhoer and V. E. Zakharov, Zh. Eksp. Teor. Fiz. **58**, 903 (1979) [Sov. Phys. JETP **31**, 486 (1970)]; M. R. Gupta, B. K. Som, and B. Dasgupta, J. Plasma Phys. **25**, 499 (1981).
[9] M. V. Tratnik and J. E. Sipe, Phys. Rev. A **38**, 2011 (1988).
[10] D. N. Christodoulides and R. I. Joseph, Opt. Lett. **13**, 53 (1988).
[11] N. N. Akhmediev, V. M. Eleonskii, N. E. Kulagin, and L. P. Shil'nikov, Pis'ma Zh. Tekh. Fiz. **15**, 19 (1989) [Sov. Tech. Phys. Lett. **15**, 587 (1989)].
[12] V. M. Eleonskii, V. G. Korolev, N. E. Kulagin, and L. P. Shil'nikov, Zh. Eksp. Teor. Fiz. **99**, 1113 (1991) [Sov. Phys. JETP **72**, 619 (1991)].
[13] S. Trillo, S. Wabnitz, E. M. Wright, and G. I. Stegeman, Opt. Lett. **13**, 871 (1988).
[14] D. N. Christodoulides, Phys. Lett. A **132**, 451 (1988).
[15] Yu. S. Kivshar and S. K. Turitsyn, Opt. Lett. **18**, 337 (1993).
[16] P. D. Maker and R. W. Terhune, Phys. Rev. A **137**, 801 (1965).
[17] E. A. Kuznetsov and S. K. Turitsyn, Zh. Eksp. Teor. Fiz. **91**, 591 (1988) [Sov. Phys. JETP **67**, 1583 (1988)].
[18] H. T. Tran, Phys. Rev. A **46**, 7319 (1992).
[19] A. W. Snyder and J. D. Love, *Optical Waveguide Theory* (Chapman and Hall, New York, 1983).
[20] R. de la Fuente and A. Barthelemy, IEEE J. Quantum Electron. **QE28**, 547 (1992).
[21] J. M. Hickmann, A. S. L. Gomes, and C. B. de Araujo, Phys. Rev. Lett. **68**, 3547 (1992).
[22] V. E. Zakharov and A. V. Mikhailov, Pis'ma Zh. Eksp. Teor. Fiz. **45**, 279 (1987) [JETP Lett. **45**, 348 (1987)].
[23] A. E. Kaplan, Opt. Lett. **8**, 560 (1983).
[24] Yu. S. Kivshar, Phys. Rev. Lett. **70**, 3055 (1993); Phys. Rev. B **46**, 8652 (1992).
[25] B. Denardo, A. Larraza, S. Putterman, and P. Roberts, Phys. Rev. Lett. **69**, 597 (1992); S. Putterman and P. Roberts, Proc. R. Soc. London, Ser. A **440**, 135 (1993).